Mon. Not. R. Astron. Soc. **365,** 127–133 (2006) doi:10.1111/j.1365-2966.2005.09693.x

WR 143: a Wolf–Rayet binary

Watson P. Varricatt[1]★ and Nagarhalli M. Ashok[2]★

[1]*Joint Astronomy Center, 660 N. Aohoku Place, Hilo, Hawaii 96720, USA*
[2]*Physical Research Laboratory, Navrangpura, Ahmedabad, 380009, India*

Accepted 2005 September 29. Received 2005 September 24; in original form 2005 June 21

ABSTRACT

Near-infrared spectroscopy and photometry of the Wolf–Rayet star WR 143 (HD 195177) were obtained in the *JHK* photometric bands. High-resolution spectra observed in the *J* and *H* bands exhibit a narrow 1.083-μm He I line and the H I Paβ and Brackett series lines in emission superposed on the broad emission-line spectrum of the Wolf–Rayet star, giving strong indications of the presence of a companion. From the narrow emission lines observed, the companion is identified to be an early-type Be star. The photometric magnitudes exhibit variations in the *JHK* bands, which are probably due to the variability of the companion star. The flux density distribution is too steep for a Wolf–Rayet atmosphere. This is identified to be mainly due to the increasing contribution from the early-type companion star towards shorter wavelengths.

Key words: binaries: spectroscopic – stars: emission-line, Be – stars: individual: WR 143 – stars: winds, outflows – stars: Wolf–Rayet.

1 INTRODUCTION

During the late stages of evolution, massive stars (with $M \geqslant 30\,M_{\odot}$) go through the Wolf–Rayet (WR) phase. At this stage, they are subjected to large-scale mass loss ($\dot{M} \sim 10^{-5}\,M_{\odot}\,yr^{-1}$) through accelerated stellar winds with terminal velocities in the range 750–5000 km s^{-1}. Consequently, these objects are characterized by infrared (IR) excess and strong, broad emission lines originating in their fast winds. Based on the emission lines observed, they are classified into WN, WC and WO stars. WN stars show lines of He and N in their winds, with evidence of H in the late types, and WC and WO stars show lines of He, C and O. The star WR 143 (HD 195177) is an interesting member of the WC4 type, its lines being weaker than the rest of the members of its class.

Early studies classified WR 143 as WC5+(OB) (Smith 1968). The possibility of the presence of a companion star was considered since its emission lines were weaker than those of many other stars of the same WR type, even though no absorption lines were detected. Smith, Shara & Moffat (1990a) reclassified WR 143 as a WC4 star. Figer, McLean & Najarro (1997) observed the *K*-band spectrum. They also noticed that the IR emission lines of WR 143 were weaker and broader compared to those of the other WC5-type stars, WR 111 and WR 114. The VIIth Catalogue of Galactic Wolf–Rayet Stars (van der Hucht 2001) lists WR 143 as WC4+OB?. Considering the absolute *v* magnitude of the system, van der Hucht (2001) proposed a B0V companion to the WR star in WR 143. The exact nature of the companion is not yet understood. The object is very faint at radio and X-ray wavelengths. The 6-cm radio continuum survey of Abbott et al. (1986) using the VLA gave an upper limit of the flux of 0.4 mJy, which was above their 3σ noise. However, the 3.6-cm radio continuum survey of Cappa, Goss & van der Hucht (2004) using the VLA did not detect WR 143. They derived an upper limit for its mass-loss rate to be $0.7 \times 10^{-5}\,M_{\odot}\,yr^{-1}$. WR 143 may have been detected (2σ) in the *ROSAT* X-ray survey (Pollock, Haberl & Corcoran 1995).

WR 143 is located close to the Galactic plane at a distance of −1 pc (van der Hucht et al. 1988). The distance estimates by different investigators agree quite well. From the spectroscopic parallax, Conti & Vacca (1990) estimated a heliocentric distance of 1.0 kpc, which is close to the value of 0.82 kpc estimated by van der Hucht et al. (1988) and 1.17 kpc by Smith, Shara & Moffat (1990b) using the line flux method. van der Hucht et al. (1988) estimated the extinction $A_v = 6.07$, which gives $A_V = 5.47$ assuming $A_v/A_V = 1.11$ (van der Hucht 2001).

2 OBSERVATIONS AND DATA REDUCTION

We observed the near-IR *JHK* spectra of WR 143 with the 3.8-m United Kingdom Infrared Telescope (UKIRT), and the Cooled Grating Spectrometer (CGS4) (Mountain et al. 1990) using the 40 line mm^{-1} grating. This grating, with a one-pixel slit, gives a resolution of ∼940 in the *J* band in the second order and ∼680 and ∼900 in the *H* and *K* bands, respectively, in the first order. The *J*-band spectra were taken on three epochs. Krypton, xenon and argon arc lamp spectra were used to wavelength-calibrate the *J*-, *H*- and *K*-band spectra, respectively. Table 1 gives the details of the spectroscopic observations. Fig. 1 shows the observed *J*-band spectra and Fig. 2 the *H*- and *K*-band spectra. Many narrow emission features

★E-mail: w.varricatt@jach.hawaii.edu (WPV); ashok@prl.ernet.in (NMA)

Table 1. Spectroscopic observations using UKIRT.

λ (μm)	Grating/ grism[a]	Resolution (λ/Δλ)	UT date (yyyymmdd.ddd)	Comparison star
1.083	echelle	20700	20011029.221	BS 8170
1.18	40 line mm^{-1}	944	20010613.568	BS 7756, BS 8788
1.18	40 line mm^{-1}	944	20010704.424	BS 7793
1.18	40 line mm^{-1}	944	20011029.368	BS 8170
1.70	40 line mm^{-1}	680	20010614.553	BS 7793
2.25	40 line mm^{-1}	900	20010614.625	BS 7793
1.237	long_J[a]	4100	20030619.418	BS 7672
1.522	short_H[a]	3800	20030619.435	BS 7672
1.702	long_H[a]	4000	20030812.415	BS 7672

[a]Observed using UIST. The rest were observed using CGS4.

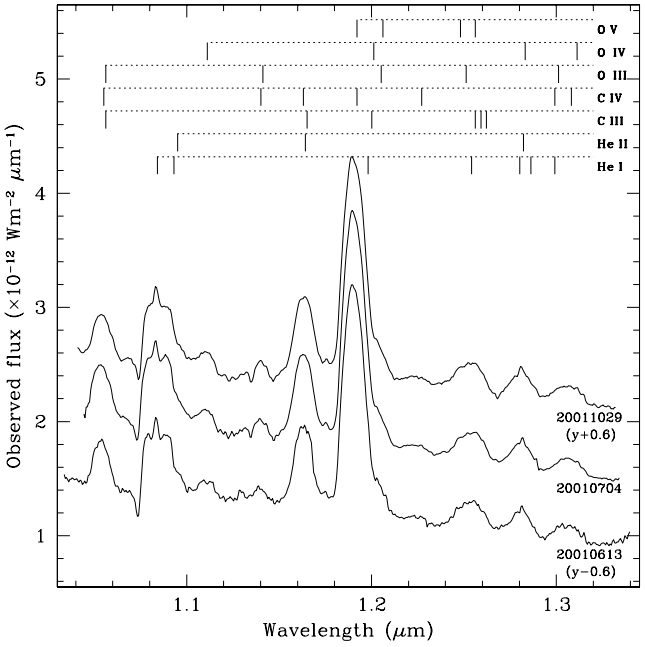

Figure 1. The observed *J*-band spectra of WR 143. Spectra are labelled by the UT dates of the observations. All spectra are plotted with the same scale, with those of 20010613 and 20011029 vertically shifted for clarity.

were observed in our *JHK* spectra. To understand these better, we again observed at higher spectral resolution at these wavelengths.

Our *J*-band spectra on all three epochs exhibited a prominent narrow emission component superposed on the broad He I emission line from the WR star at 1.083 μm. To investigate this feature, we carried out high-resolution observations with CGS4 using the echelle grating and a two-pixel slit, at a spectral resolution of ∼20700. Six wavelength settings with the echelle grating gave a reasonably good coverage of the 1.083-μm He I line, although a part of the red wing could not be covered. The observed spectrum is shown in Fig. 3. The wavelength calibration was carried out using the photospheric absorption lines of the comparison star. Heliocentric corrections were applied. The narrow emission component has an asymmetric profile and its central wavelength is seen very close to the line centre of the broad emission line from the WR star. The low-resolution *J*-band spectra taken over the three epochs with a period of five months do not show any noticeable shift in the location of the narrow emission component. Visual inspection shows that this emission was also present at nearly the same wavelength in the spectrum presented by Eenens & Williams (1994). There is a conspicuous narrow absorption seen at 10778 Å, which is not identified. From the well-defined blue edge of the P Cyg absorption profile of the line, we estimate a $V_{\rm edge} = 2845 \pm 15$ km s^{-1}. This is close to the value of $V_\infty = 2750$ km s^{-1} observed by Eenens & Williams (1994).

The 1.281-μm He II line also exhibited a faint narrow emission component close to the line centre. Some of the lines from 1.55 to 1.681 μm were also observed to be much narrower than the rest of the WR lines. Observations were again carried out using UKIRT and UIST (Ramsay Howat et al. 2000) at higher spectral resolution ($R \sim 4000$) to resolve the narrow emission lines better. The UIST spectra were wavelength-calibrated using an argon arc lamp mounted inside the instrument. These spectra show the H I Paβ and the Br series lines superposed on the broad emission-line spectrum of the WR star. Fig. 4 shows the observed spectra in the *JH* bands.

All the spectroscopic observations were carried out by nodding the telescope on two positions separated by ∼12 arcsec along the slit. The flat-field observations were obtained by exposing the arrays to blackbodies mounted inside the instruments. Preliminary reduction of the data including co-adding the frames and the bias and the flat-field corrections were carried out using ORACDR, the pipeline reduction facility at UKIRT. The spectra were optimally extracted using the Starlink software FIGARO. Comparison stars (listed in Table 1) were observed at all wavelength settings. The observed comparison star spectra were corrected for their photospheric temperatures by dividing by appropriate blackbodies, and their photospheric hydrogen absorption lines were interpolated across and removed at the continuum level before ratioing the object spectra with them. The final reduction, involving the calculations of the line fluxes and the equivalent widths (EWs), were carried out using IRAF.

Photometry in the *JHK* bands was acquired on three epochs from 2001 March to 2002 December using the 1.2-m Mt. Abu Infrared Telescope and a liquid nitrogen cooled 256 × 256 NICMOS3 IR array. FS 149 and 150, two of the UKIRT faint standard stars (Hawarden et al. 2001), were observed for calibration. Observations were carried out by dithering the object on several positions on the array. The dark observations were obtained before each set of the on-sky observations and the flat-field corrections were applied using the flat fields generated from the object observations by median-combining the observed frames. The observed *JHK* magnitudes are shown in Table 2 along with the 2MASS magnitudes and the other near-IR photometric measurements available.

The observed spectra were flux-calibrated using the average *JHK* magnitudes of the three epochs of our observations. The strong emission lines present in the photometric bands contribute significantly to the observed magnitudes. Hence, the magnitudes were corrected to subtract out the contribution from the emission lines adopting a method similar to Eenens & Williams (1992). The equivalent widths (EWs) of the emission lines were estimated from the ratioed spectra; these EWs were weighted with the transmission of the filters used in the Mt. Abu photometry and the corrections for the lines were derived as

$$\Delta_{\rm mag} = 2.5 \log \frac{\rm LW + FW}{\rm FW},$$

where FW is the bandwidth of the filter used for the photometry and LW is the sum of the weighted EWs of the emission lines within the photometric band. $\Delta_{\rm mag}$ were added to the observed magnitudes to obtain the magnitudes representing the continua, which were then used to flux-calibrate the observed *JHK* spectra.

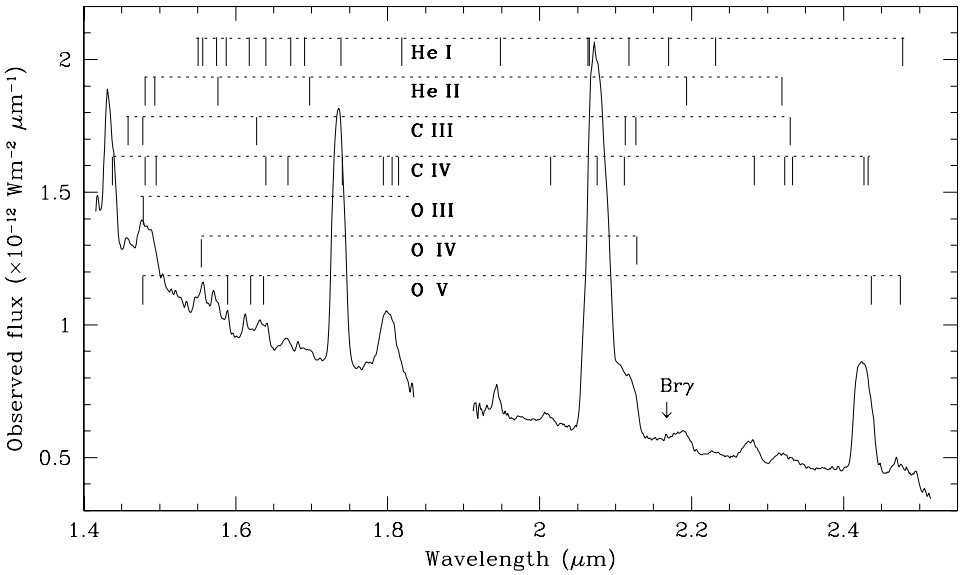

Figure 2. The observed *H*- and *K*-band spectra of WR 143. The gap shows the region of strong telluric absorption.

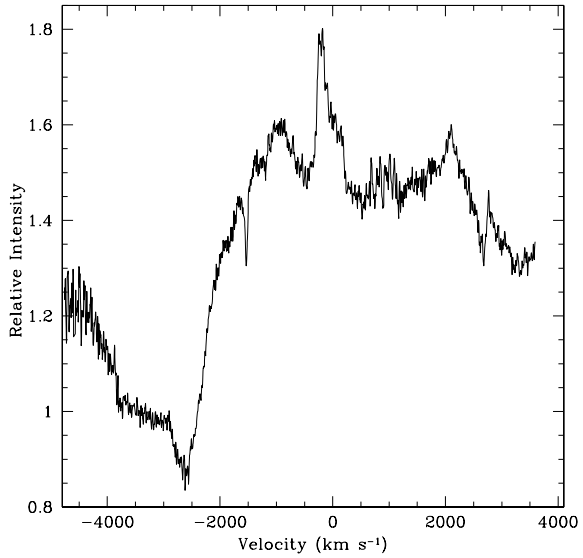

Figure 3. The echelle spectrum of the 1.083-μm He I line. Velocities are given with respect to the line centre.

The spectra were dereddened assuming $A_V = 5.47$ with an interstellar reddening law with $R_V = A_V/E(B-V) = 3.1$. Line fluxes and equivalent widths of the emission lines are estimated from the dereddened spectra. The *J*-band spectra of the three epochs were averaged before estimating the equivalent widths. The lines were fitted with Gaussian profiles for estimating the EWs and full width at half-maximum (FWHM). Multiple Gaussians were fitted when there was line blending. For the strongly blended lines, we give only the the equivalent widths of the combined profiles; the FWHM of the individual components are not listed in those cases. The lines identified, their fluxes and the equivalent widths are shown in Table 3. The line identifications are adopted from Eenens, Williams & Wade (1991) and from the atomic line list of Peter van Hoof.[1] The arc lines observed using the UIST high-resolution grisms showed an average FWHM of 75 km s^{-1}. The FWHM of the narrow emission lines measured in these spectra have been corrected to account for this. The identifications, FWHMs, fluxes and EWs of the narrow emission lines are listed in Table 4. The estimates for the broad WR emission lines from these high-resolution spectra are listed in Table 3. Most of the errors in the line fluxes and the EWs arise from the accuracy with which the continuum is defined. Hence, the errors are determined by multiple measurements of these values on any specific line or blend. The values given in Tables 3 and 4 are the averages of eight independent determinations from the dereddened spectra. The 1σ standard deviations are given in brackets against the line fluxes and the EWs.

[1] P. A. M. van Hoof, http://star.pst.qub.ac.uk/∼pvh/

3 DISCUSSION AND CONCLUSIONS

Table 2 and Fig. 5 show the variability of the *JHK* magnitudes. The *JHK* magnitudes measured by us on the three epochs (within ∼21 months) did not exhibit any significant variability beyond the observational errors. However, these three measurements are consistently brighter than the 2MASS *JHK* magnitudes observed 3 yr prior to our first measurement by ∼0.45 mag. To verify if this is genuine, we measured the *JHK* magnitudes of two other stars in our images and compared those with the 2MASS measurements and found a good agreement. Hence, the brightening that we observe in our photometry compared to 2MASS could indicate a genuine brightening of one of the stars in the WR 143 binary.

From the dereddened spectra, we estimated the ratios of the equivalent widths of the emission lines (1.083+1.094)/(1.191+1.199) and (1.693+1.701)/1.736 to be 0.38 and 0.03, respectively, which are consistent with a WC type earlier than WC5 when compared with the line ratios estimated by Eenens et al. (1991). The ratios 1.28/(1.083+1.094), 2.08/2.11 and 2.43/2.48 are 0.28, 5.7 and 3.5, respectively, which are somewhat less than for a WC4 star. However, the line ratios estimated by Eenens et al. (1991) extend down only to WC5 type and have only one or two objects per WC type, and hence we do not know about the uncertainty in these ratios. In general, our *JHK* spectra agree with a WC4 type for this star.

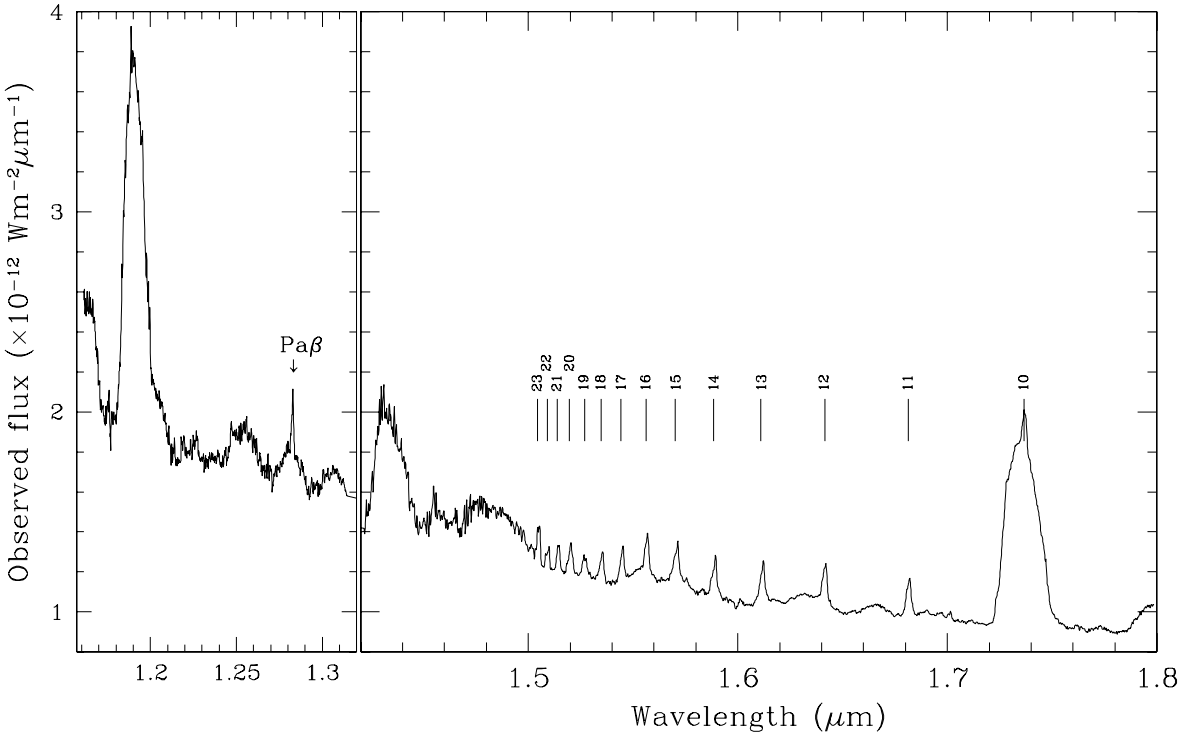

Figure 4. High-resolution spectrum of WR 143 observed using UIST. The upper levels of the H I Br series lines are indicated against the lines as numbers.

Table 2. The near-IR photometric data.

Place	Date	*J*	*H*	*K*	*L*
Mt. Abu	2002 December 15	8.18 (0.06)	7.61 (0.03)	6.99 (0.05)	
Mt. Abu	2002 December 14	8.13 (0.04)	7.63 (0.05)	7.05 (0.05)	
Mt. Abu	2001 March 28	8.15 (0.04)	7.65 (0.04)	7.09 (0.07)	
2MASS	1998 June 21	8.59 (0.01)	8.10 (0.01)	7.46 (0.01)	
Cohen et al. (1975)				7.50 (0.2)	7.2 (0.2)
Allen et al. (1972)			7.96	7.34	

WR 143 was detected by the MSX at 8.28 μm (Egan et al. 2003) with a flux density of 0.1285 mJy. Observations at 10 μm by Cohen, Barlow & Kuhi (1975) and Smith & Houck (2001) differ very much and are only upper limits. Hence those are not considered here. The near-IR magnitudes given in Table 2 and the line free magnitudes reported by Massey (1984) (13.97, 13.16, 11.95 and 11.17 mag, respectively, in the narrow-band *u*, *b*, *v* and *r* filters) are dereddened adopting the value of $A_V = 5.47$ and following the extinction relations given by Cardelli, Clayton & Mathis (1989). Fig. 5 shows the flux density distribution of WR 143 from 0.365 to 8.28 μm. At radio and infrared wavelengths, the flux density distribution (S_ν) of a uniform, ionized, spherically symmetric wind can be represented by a power law of the form $S_\nu \propto \nu^\alpha$ with $\alpha = 0.6$, where ν is the frequency of observation (Wright & Barlow 1975). This value of α is intermediate between $\alpha = -0.1$, expected for free–free emission from an optically thin homogeneous plasma, and $\alpha = 2.0$, expected for that from an optically thick plasma. Williams (1999) estimated an average value of $\alpha = 0.7$ from millimetre and radio observations. The observed values of α at shorter wavelengths are somewhat higher since the radiation at these wavelengths is mainly emitted from the inner regions where the wind is still being accelerated. Morris et al. (1993) found that, in the wavelength interval ∼0.14–1.0 μm, the continuum energy distribution can be represented by a power law with mean $\alpha = 0.85 \pm 0.26$. Setia Gunawan (2001) estimates an average value of $\alpha = 1.21 \pm 0.24$ from the optical and near-IR (also MSX, mm and radio data for some objects) of nine non-dusty WR stars. The average of α for six single WR stars given in Setia Gunawan (2001) gives 1.13 ± 0.24. A linear least-squares fit to all the observed data of WR 143 from 0.36 to 8.28 μm (continuous line in Fig. 5) gives $\alpha = 1.73$ ($1\sigma = 0.06$). In Fig. 5, we have also plotted the power-law flux density distribution for $\alpha = 1.13$ (dotted line), scaled to match our fitted line at 1.25 μm. We see that, for WR 143, the flux density distribution is much steeper than what is seen for most of the WR stars. We propose that the much steeper slope of the spectral energy distribution of WR 143 is due to the increasing contribution of the early B-type companion star towards shorter wavelengths. A linear fit, when forced through the 0.36–3.6 μm region of a B0V star, gives $\alpha = 1.77$.

The presence of the narrow emission lines in our spectra gives us additional clues about the nature of the companion star of WR 143. Most Be stars in their emission phase show Br series lines in the *H* and *K* bands (Clark & Steele 2000; Steele & Clark 2001). Be

Table 3. Line identifications, equivalent widths, line fluxes and FWHM estimated from the dereddened spectra. A half-line blank space separates the blends. 1σ errors are shown in brackets. Linestrengths estimated from the high-resolution spectra are shown by '$*$'. The rest are from the low-resolution spectra.

λ (μm)	Main contributor	Other possible contributors	Flux (10^{-15} W m^{-2})	EW (Å)	FWHM (km s^{-1})
1.054	C IV (12–9)	1.055 (C III); 1.055 (O III)	28 (0.8)	−21 (0.6)	2715 (43)
1.083 + 1.092 + 1.094	He I (2p–2s); He I (6f–3d); He II (12–6)		64.3 (0.5)	−54.5 (0.5)	
1.11	O IV (3p–4f)	1.1–1.101 (He I)	11.7 (0.6)	−12.6 (0.6)	3340 (112)
1.139	C IV (8d–7p)	1.14 (O III)	6.5 (0.4)	−6.6 (0.4)	
1.163 + 1.162–1.163 + 1.164	He II (7–5); C IV (14–10); C III (7d–6p)		48 (0.8)	−53 (1)	3070 (140)
1.191 + 1.198–1.199	C IV (8–7); C III (4p–4s)	1.191 (O V); 1.197 (He I)	123 (3)	−145 (4)	
1.205	O V (2p4d–2p4p)	1.20 (O IV); 1.2–1.209 (O III)	17 (0.6)	−20.7 (0.6)	2845 (30)
1.226	C IV (8p–7d)		3 (0.5)	−3.9 (0.7)	2670 (78)
1.255–1.26	C III (7f–6d, 9–7)	1.253 (He I); 1.258, 1.261 (C III); 1.247, 1.255 (O V); 1.25 (O III)	16.6 (0.2)	−23.6 (0.3)	
1.281 + 1.279, 1.285	He II (10–6); He I (5–3)	1.282 (O IV)	10 (0.2)	−15.4 (0.3)	2530 (25)
1.298, 1.307	C IV (8s–7p, 16–11)	1.297, 1.299 (He I); 1.3 (O III); 1.31 (O IV)	7.8 (0.4)	−13 (0.7)	
1.435	C IV (4p–4s)		23 (1)	−54.7 (2.7)	2800 (33)
1.454	C III (7g–6f)		1.6 (0.2)	−4.2 (0.6)	1950 (123)
1.476	He II (9–6)	1.474 (O III); 1.473 (O V); 1.473 (C III); 1.476 (C IV)	6.5 (0.2)	−17.8 (0.5)	
1.489 + 1.490, 1.491	He II (14–7); C IV (15f–11d, 15g–11f)		5.6 (0.3)	−16.1 (0.8)	
*1.546, 1.552	He I (11–4, 13–4)	1.55 (O IV)	3.8 (0.1)	−13.6 (0.3)	
*1.570 + *1.572	He I (15–4); He II (13–7)		2.1 (0.1)	−7.7 (0.2)	
*1.579, 1.587	He I (12–4, 14–4)	1.58–1.587 (O V)	1.04 (0.2)	−4 (0.7)	
*1.616, 1.61	He I (11–4, 13–4)	1.61, 1.619 (O V)	0.83 (0.1)	−3.4 (0.5)	
*1.623 + *1.635	C III (7p–6d); C IV (17–12)	1.63–1.64 (He I); 1.632 (O V)	3.9 (0.2)	−16.4 (0.6)	
*1.664	C IV (9d–8p)	1.668 (He I)	1.4 (0.1)	−6.1 (0.4)	
*1.693	He II (12–7)	1.681–1.701 (He I)	1.3 (0.2)	−6.2 (0.8)	
1.732–1.740	C IV (9–8)	1.734 (He I)	40.8 (0.5)	−208 (3)	2870 (12)
1.790, 1.801	C IV (9–8, 14–11)	1.81 (C IV); 1.814 (He I)	16.8 (0.5)	−95.7 (2.9)	
1.944	He I (8–4)		2.0 (0.03)	−15.2 (0.3)	1450 (19)
2.010	C IV (18–13)		1.1 (0.1)	−8.5 (0.8)	
2.071 + 2.059	C IV (3d–3p); He I (2p–2s)	2.061 (He I)	80.9 (0.3)	−729 (4)	
2.108, 2.122 + 2.113	C III (5p–5s, 4d–4p); He I (4s–3p)	2.107 (C IV); 2.123 (O IV)	13.6 (0.4)	−129 (4)	
2.165	He I (7–4)		2.2 (0.2)	−22.3 (2)	
2.189	He II (10–7)		2.7 (0.2)	−28.9 (2)	
2.227	He I (7s–4p)		0.79 (0.15)	−9.04 (1.7)	
2.278	C IV (15–12)		2.86 (0.1)	−34 (1)	2755 (40)
2.318	C IV (17–13)	2.314 (He II); 2.323–2.327 (C III); 2.328 (C IV)	1.7 (0.05)	−21 (0.6)	
2.423–2.427 + 2.422–2.433	C IV (13–11); C IV (10–9)	2.432 (O V)	18.4 (0.3)	−259 (5)	
2.473	He I (6d–4p)	2.470 (O V)	4.6 (0.2)	−74 (4)	

Table 4. Narrow emission lines.

λ observed (μm)	Identification	Flux (10^{-16} W m^{-2})	EW[a] (Å)	FWHM (km s^{-1})
Hydrogen lines				
1.2827	5–3	1.5 (0.1)	−2.2 (0.1)	306 (7)
1.50495	23–4			
1.50938	22–4	5.1 (0.1)	−1.6 (0.04)	389 (4)
1.51438	21–4	6.7 (0.2)	−2.1 (0.1)	334 (6)
1.52021	20–4	9.3 (0.3)	−3.0 (0.1)	465 (12)
1.52692	19–4	7.0 (0.2)	−2.3 (0.1)	511 (11)
1.53517	18–4	8.0 (0.1)	−2.7 (0.04)	418 (5)
1.54485	17–4	8.6 (0.2)	−2.9 (0.1)	407 (6)
1.55665	16–4	9.9 (0.3)	−3.3 (0.1)	395 (11)
1.57082	15–4	13.7 (0.3)	−4.8 (0.1)	591 (11)
1.58895	14–4	12.4 (0.5)	−4.7 (0.2)	539 (15)
1.61179	13–4	12.6 (0.2)	−5.1 (0.1)	515 (5)
1.64153	12–4	12.4 (0.3)	−5.1 (0.1)	485 (8)
1.68164	11–4	11.6 (0.2)	−5.3 (0.1)	484 (5)
1.73678	10–4	8.3 (0.4)	−2.1 (0.1)	339 (14)
2.166	7–4, detected in the low-resolution spectrum			
Helium line				
1.083	$2p^3P$–$2s^3S$	3.6 (0.1)	−2.4 (0.1)	

[a]Will be strongly affected by the Wolf–Rayet continuum and the broad emission lines.

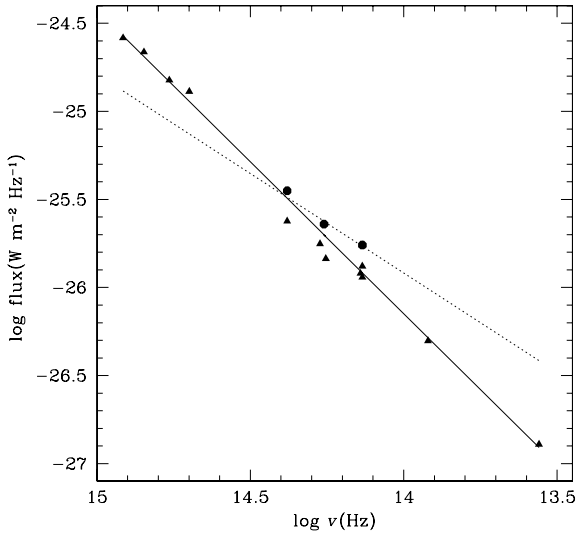

Figure 5. Flux density distribution of WR 143. Filled circles show our *JHK* measurements with the measurements on different epochs averaged, and the filled triangles show observations by others. The full line shows a linear least-squares fit to the data, which gives $\alpha = 1.72$ and the dotted line is the distribution with $\alpha = 1.13$, the average for six single WR stars from the list of Setia Gunawan (2001), scaled to match our fitted line at 1.25 μm.

stars with spectral type earlier than B2.5 also exhibit the He I line at 2.058 μm in emission (Clark & Steele 2000). For WR 143, this wavelength is blended with the broad C IV and C III emission lines of the WR star; therefore we cannot conclude anything about its presence in the spectrum of the companion. However, the narrow emission component on the broad 1.083-μm He I emission line close to the line centre is stable over the epochs of our observation. This feature is clearly seen in all the published near-IR spectra of WR 143 and is identified as the He I emission line from the companion. A prominent 1.083-μm emission line has been observed in early-type Be stars before (Lowe et al. 1985). H I Brackett series emission lines are exhibited by most of the Be stars in their emission phase. However, the additional presence of the He I emission line shows that the companion is a Be star of spectral type earlier than B2.5.

The spectrum of WR 143 appears to undergo long-term variations. The equivalent width of the 1.083-μm He I line measured from our spectra is 54.5 ± 0.5 Å, which differs from the 61 Å measured by Kuhi (1968) and 32 Å observed in 1989 September (Vreux, Andrillat & Biemont 1990). The optical spectrum of WR 143 was observed by Torres & Massey (1987). We obtained their published spectrum from the CDS Service for Astronomical Catalogues and examined it. The He II, C IV blend at 6564 Å appears to have a sharper peak compared to the other optical emission lines of WR 143, indicating the possible presence of Hα in emission superposed on this blend. However, it should be noted that we did not see the Hβ and Hγ lines in their spectrum. The equivalent widths of most of the emission lines are much weaker in the *K*-band spectrum observed by us compared to those observed by Figer et al. (1997). We cannot say how much of these variations mentioned above are due to the differences in the measurement techniques. However, from the difference in the equivalent widths between our results and the recent measurements of Figer et al. (1997), where both used the same technique, we can consider some to be genuine. For the C IV blends at 2.071 and 2.278 μm, we measure EWs of 729 and 34 Å, respectively, whereas Figer et al. obtained 1069 and 59 Å, respectively.

To understand if these could be produced by the brightening that we see in our photometry, we assumed a disc of $T_{\rm eff} = 18\,000$ K, appropriate for a disc around an early-type Be star (Waters 1986), as the cause of the current brightening in the near-IR photometry. A 18 000 K blackbody curve was subtracted from our flux-calibrated *K*-band spectrum. The flux of the blackbody was scaled so that, when subtracted, the flux of the subtracted spectrum agreed with that of the observed spectrum calibrated with the 2MASS *K*-band photometry at the band centre. The equivalent widths of the lines at 2.071 and 2.278 μm, measured from the subtracted spectrum, gave 1012 and 52 Å, respectively, showing that the lower EW measured from our spectra compared to that reported by Figer et al. (1997) is most probably due to a brightening of the Be star companion star, resulting in an increase in the continuum flux. Be stars are known to exhibit variability (Dougherty & Taylor 1994).

Other than early-type Be stars, a variety of early-type objects like Ofpe/WN9 stars and luminous blue variables exhibit H I Pa and Br series emission lines and He I lines (Morris et al. 1996; Bohannan & Crowther 1999). However, these objects are much more luminous than the $M_v = -3.66$ for the companion derived by van der Hucht (2001), which is typical of early-type B and Be stars (Wegner 2000). Hence, we conclude that the companion is an early-type Be star. Since Be stars are known to vary, the photometric variations observed must be due to the variability of the Be star companion.

ACKNOWLEDGMENTS

UKIRT is operated by the Joint Astronomy Center, Hilo, on behalf of the UK Particle Physics and Astronomy Research Council (PPARC). The Mt. Abu Observatory is operated by the Physical Research Laboratory, Ahmedabad, funded by the Department of Space, Government of India. We would like to thank the UKIRT service programme for obtaining some of the spectra and the staff members of UKIRT and Mt. Abu observatories for helping us with the data collection. This publication makes use of data products

from the Two Micron All Sky Survey, which is a joint project of the University of Massachusetts and the Infrared Processing and Analysis Center/California Institute of Technology. We thank Peredur Williams for his comments and suggestions, which have improved the paper. Several of the software packages developed by the Starlink project run by CCLRC on behalf of PPARC and IRAF developed at NOAO are used for reducing the data. This research has also made use of the Simbad data base operated by CDS, Strasbourg, France, and the NASA ADS data base, hosted by the Harvard–Smithsonian Center for Astrophysics.

REFERENCES

Abbott D. C., Bieging J. H., Churchwell E., Torres A. V., 1986, ApJ, 303, 239
Allen D. A., Swing J. P., Harvey P. M., 1972, A&A, 20, 333
Bohannan B., Crowther P. A., 1999, ApJ, 511, 374
Cappa C., Goss W. M., van der Hucht K. A., 2004, AJ, 127, 2885
Cardelli J. A., Clayton G. C., Mathis J. S., 1989, ApJ, 345, 245
Clark J. S., Steele I. A., 2000, A&AS, 141, 65
Cohen M., Barlow M. J., Kuhi L. V., 1975, A&A, 40, 291
Conti P. S., Vacca W. D., 1990, AJ, 100, 431
Dougherty S. M., Taylor A. R., 1994, MNRAS, 269, 1123
Eenens P. R. J., Williams P. M., 1992, MNRAS, 255, 277
Eenens P. R. J., Williams P. M., 1994, MNRAS, 269, 1082
Eenens P. R. J., Williams P. M., Wade R., 1991, MNRAS, 252, 300
Egan M. P. et al., 2003, Air Force Research Laboratory Technical Report AFRL-VS-TR-2003-1589
Figer D. F., McLean I. S., Najarro F., 1997, ApJ, 486, 420
Hawarden T. G., Leggett S. K., Letawsky M. B., Ballantyne D. R., Casali M. M., 2001, MNRAS, 325, 563
Kuhi L. V., 1968, in Gebbie K. B., Thomas R. N., eds, Wolf–Rayet Stars, NBS SP-307, p. 101
Lowe R. P., Moorhead J. M., Wehlau W. H., Baker P. K., Malborough J. M., 1985, ApJ, 290, 325
Massey P., 1984, ApJ, 281, 789
Morris P. W., Brownsberger K. R., Conti P. S., Massey P., Vacca W. D., 1993, ApJ, 412, 324
Morris P. W., Eenens P. R. J., Hanson M. M., Conti P. S., Blum R. D., 1996, ApJ, 470, 597
Mountain C. M., Robertson D. J., Lee T. J., Wade R., 1990, in Crawford D. L., ed., Proc. SPIE, Vol. 1235, Instruments in Astronomy VII. SPIE, Bellingham, WA, p. 25
Pollock A. M. T., Haberl F., Corcoran M. F., 1995, in van der Hucht K. A., Williams P. M., eds., Proc. IAU Symp. 163, Wolf–Rayet Stars: Binaries; Colliding Winds; Evolution. Kluwer, Dordrecht, p. 512
Ramsay Howat S. K., Ellis M. A., Gostick D. C., Hastings P. R., Strachan M., Wells M., 2000, in Iye M., Moorwood A. F., eds, Proc. SPIE, Vol. 4008, Optical and IR Telescope Instrumentation and Detectors. SPIE, Bellingham, WA, p. 1067
Setia Gunawan D. Y. A., 2001, PhD thesis, Univ. Groningen
Smith J. D. T., Houck J. R., 2001, AJ, 121, 2115
Smith L. F., 1968, MNRAS, 138, 109
Smith L. F., Shara M. M., Moffat A. F. J., 1990a, ApJ, 348, 471
Smith L. F., Shara M. M., Moffat A. F. J., 1990b, ApJ, 358, 229
Steele I. A., Clark J. S., 2001, A&A, 371, 643
Torres A. V., Massey P., 1987, ApJS, 65, 459
van der Hucht K. A., 2001, New Astron. Rev., 45, 135
van der Hucht K. A., Hidayat B., Admiranto A. G., Supelli K. R., Doom C., 1988, A&A, 199, 217
Vreux J.-M., Andrillat Y., Biemont E., 1990, A&A, 238, 207
Waters L. B. F. M., 1986, A&A, 162, 121
Wegner W., 2000, MNRAS, 319, 771
Williams P. M., 1999, in van der Hucht K. A., Koenigsberger G., Eenens P. R. J., eds, Proc. IAU Symp. 193, Wolf–Rayet Phenomena in Massive Stars and Starburst Galaxies. Astron. Soc. Pac., San Francisco, p. 267
Wright A. E., Barlow M. J., 1975, MNRAS, 170, 41

This paper has been typeset from a TEX/LATEX file prepared by the author.